ORNL/SPR-2019/1324

Progress Report on Length Dependence of Severe Accident Test Station Integral Testing

Nuclear Technology Research and Development

Prepared for US Department of Energy
Advanced Fuel Campaign
B. Garrison
P. A. Champlin
M. Howell
M. N. Cinbiz
M. Gussev
C. M. Petrie
K. Linton
Oak Ridge National Laboratory
M3FT-19OR020204083
September 2019

SUMMARY

The safety of accident-tolerant fuel (ATF) candidates must be tested under simulated loss-of-coolant accident (LOCA) conditions to evaluate their improved safety margins. This evaluation eventually must include testing of irradiated materials. This report describes the fiscal year (FY) 2019 activities to (1) improve the information yield of integral design–basis LOCA tests by using digital image correlation (DIC) calculations on the engraved specimens' surfaces and (2) to investigate the effects of reducing the length of nuclear-grade FeCrAl specimens tested in the Severe Accident Test Station (SATS) to improve the cost-effectiveness of irradiation campaigns for future work. Analysis showed the DIC technique to be effective at calculating strains, and that specimens as short as 4 inches could be used for LOCA experiments while maintaining similar balloon and burst behavior as 12-inch specimens.

With these results, an irradiation vehicle design effort was initiated to encapsulate multiple 4-inch thin-walled tube cladding specimens and test them under irradiation in the flux trap of the High Flux Isotope Reactor. By utilizing thermal modeling and optimizing the design parameters, calculated specimen temperatures were predicted to vary less than 2% during irradiation. Future work is planned to finalize the design and safety basis approvals and initiate a HFIR irradiation in support of in-cell integral LOCA tests at the Irradiated Fuels Examination Laboratory (IFEL).

INTENTIONALLY BLANK

CONTENTS

SUMMARY iii

ACRONYMS viii

ACKNOWLEDGMENTS ix

1. INTRODUCTION 1

2. LENGTH DEPENDENCE OF LOCA TESTS 1
   - 2.1 EXPERIMENTAL SETUP 1
   - 2.2 SATS RESULTS WITH VARYING-LENGTH SPECIMENS 5
   - 2.3 DIC TECHNIQUE WITH LASER-ENGRAVED SURFACES 7

3. IRRADIATION TARGET DESIGN 3
   - 3.1 DESIGN CONCEPT 3
   - 3.2 SETUP FOR THERMAL ANALYSIS OF IRRADIATION DESIGN 6
   - 3.3 RESULTS FROM THERMAL ANALYSIS 7

4. CONCLUSIONS 8

5. REFERENCES 9

FIGURES

Figure 1. The Severe Accident Test Station (SATS) used to simulate design-basis loss of coolant accident (LOCA) conditions at ORNL. 2

Figure 2. Typical temperature and pressure history of a design-basis LOCA event 3

Figure 3. Setup for specimens shorter than the standard 12 inches. 4

Figure 4. Burst temperature vs. burst pressure results of varying lengths of C26M2 FeCrAl SATS specimens (4-inch specimens appear to be within scatter and are still a valid specimen length). 5

Figure 5. Images and measurements of the burst openings for varied-length specimens at an initial pressure of 8.3 MPa (1,200 psi). No correlation was shown between specimen length and burst measurements. 6

Figure 6. Image of the engraving pattern used for DIC strain calculations (a), and optical microscope image showing the depth of the square engraved pattern (b). 7

Figure 7. Image of engravings and DIC selection areas on FeCrAl tube surface before SATS test (a), where the DIC software traced the selected strain-measurement locations on the post-test image (b), and hoop strain results calculated from DIC software at different tube locations relative to burst location (c). A biaxial stress state was calculated on the opposite orientation of the burst with less biaxiality at the burst location 2

Figure 8. Design of the cladding irradiation experiment performed in HFIR at ORNL. 3

Figure 9. Cross sections of the new cladding specimen assembly design incorporated in the irradiation experiments shown in Figure 8. Note that the disks are hidden in the top-down section for clarity. 4

Figure 10. Tapered profile of the Al holder accounting for temperature changes from the power generation profile by decreasing the holder OD to improve thermal conductivity. 5

Figure 11. Temperatures (in °C) of the FeCrAl cladding tube specimens during HFIR irradiation using the new target design (results obtained from ANSYS simulations) 7

TABLES

Table 1. Composition of the nuclear-grade C26M FeCrAl cladding tubes used in this work. 2

Table 2. Cladding tube irradiation materials and material property references 6

Table 3. Optimized holder diameters (inputs) and FeCrAl specimen temperatures (outputs) for ANSYS simulations 7

Table 4. Cladding tube irradiation thermal boundary conditions 7

ACRONYMS

ATF	accident-tolerant fuel
LOCA	loss-of-coolant accident
DAC	Design and Analysis Calculation
DIC	digital image correlation
DOE	US Department of Energy
FeCrAl	iron-chromium-aluminum alloy
EBSD	electron backscatter diffraction
HFIR	High Flux Isotope Reactor
HGR	heat generation rate
IFEL	Irradiation Fuels Examination Laboratory
LWR	light-water reactor
OD	outer diameter
ORNL	Oak Ridge National Laboratory
SATS	Severe Accident Test Station
TC	thermocouple
TREAT	Transient Reactor Test [facility]

ACKNOWLEDGMENTS

This work was supported by the US Department of Energy Office of Nuclear Energy (DOE-NE) Advanced Fuels Campaign (AFC). The authors thank Bruce Pint of ORNL for use of the SATS and Keyence microscope facilities.

TUBE LENGTH DEPENDANCE DURING SIMULATED LOCA TESTING IN THE SEVERE ACCIDENT TEST STATION

1. INTRODUCTION

The performance of accident-tolerant fuel (ATF) candidates must be evaluated under simulated loss-of-coolant accident (LOCA) conditions to support licensing of these materials [1-7]. The cladding integrity is a primary focus of safety testing and remains a significant research priority for the Advanced Fuels Campaign. Integral fuel safety testing ranges from separate-effects tests to simulated LOCA testing using electrical heating to in-pile tests at the Idaho National Laboratory's Transient Reactor Test (TREAT) facility [2-7]. As ATF concepts mature and undergo irradiations in commercial and test reactors, the availability of in-cell simulated-LOCA testing at the Oak Ridge National Laboratory (ORNL) Severe Accident Test Station (SATS) provides the opportunity for direct comparison with results from simulated LOCA tests previously performed on Zirconium-based light-water reactor (LWR) cladding as well as in-pile LOCA tests in TREAT. SATS testing can expose a single 12-inch cladding segment to the temperature, pressure, oxidation and water-quench conditions anticipated during a LOCA, and the high temperature module can be deployed to subject segments to beyond-design-basis-accident conditions.

With the limited irradiated ATF material available for SATS testing, the standard requirement of a 12-inch segment becomes a significant limiting factor on the amount of in-cell testing that can be performed. The cost and difficulty of irradiating such specimens in the High Flux Isotope Reactor (HFIR) continues to be a barrier to using target rod irradiations for in-cell burst testing at ORNL. If the length-dependence of SATS integral LOCA testing can be further understood, it may be possible to reduce the length requirement for test segments, which will benefit future irradiation and post-irradiation examination campaigns because the irradiation tests could accommodate a larger number of specimens. Furthermore, developing methods, such as the digital image correlation (DIC) technique, to improve the information yield of each SATS test could significantly improve the material knowledge gained for new ATF candidates and the validity of conclusions from integral test results. This report describes the efforts in proving the viability of shorter length segments, applicability of laser engraving for DIC analysis, and progress made towards their eventual irradiation in HFIR.

2. LENGTH DEPENDENCE OF LOCA TESTS

2.1 EXPERIMENTAL SETUP

The material tested in this work was as-drawn nuclear-grade FeCrAl (C26M) tubes developed at ORNL. Its composition is shown in Table 1. ORNL's SATS system shown in Figure 1 was used for the simulated-LOCA tests [4]. A Tykma Electrox Lasergear BOQX system was used to mark specimen surfaces. Burst characteristics and laser-marked pattern images for DIC analysis were taken with a Keyence VR-3100 3D measurement microscope, and metallography mounted specimens were imaged and measured with a LEICA DM2500M optical microscope.

The SATS system is designed to simulate a LOCA by increasing the temperature of an internally pressurized tube in a steam environment to what would be expected in a reactor [4,5]. Increasing temperature consequently increases the internal pressure and hoop stresses until the tube specimen eventually bursts. A typical temperature and pressure history from a SATS test is shown in Figure 32 below. Tube performance is quantified by the burst temperature, burst pressure, hoop stresses, and burst

characteristics of the tube specimen [3,4,5,7]. The standard SATS specimen [5] consists of a 12-inch cladding tube connected on both ends with Swagelok fittings so the tube can hold pressure. The standard tube is filled with Zirconia rods to maintain the thermal mass and internal gas volume similar to that of an in-reactor specimen. For shorter segments to be utilized in SATS, the pressure fittings at the ends of the segments must maintain the internal pressure during the temperature ramp and the cladding must demonstrate similar balloon and burst behavior as a 12-inch segment.

SATS specimens were tested with 4, 5, 6, 8, and 12-inch lengths at 8.3 MPa initial pressure. Specimens with a 4-inch length were found to be sufficient to induce LOCA burst, so more tests were performed at lower pressures with 4-inch tubes. To maintain a similar internal gas volume and temperature distribution in the shorter specimens during SATS tests, thick-walled Hastelloy extensions were added to the bottom and top of each tube so that the total length was 12 inches (shown in Figure 3). Thermocouples (TC)were attached to the specimen's outer surface by wrapping platinum-30% rhodium wire around the TC bead and the tube's outer diameter (OD) surface. For each specimen that was 6–12 inches long, TCs were attached to the front and back of the specimen's surface 2 inches above and below the centerline. For 5-inch specimens, TCs were attached 1.5 inches above and below centerline, and for 4-inch specimens, TCs were attached 1 inch above and below the centerline. The bottom front TC was used as the control TC, and the others were used to measure temperature. Burst location was recorded after the test, and the TC closest to the burst was used to determine burst temperature.

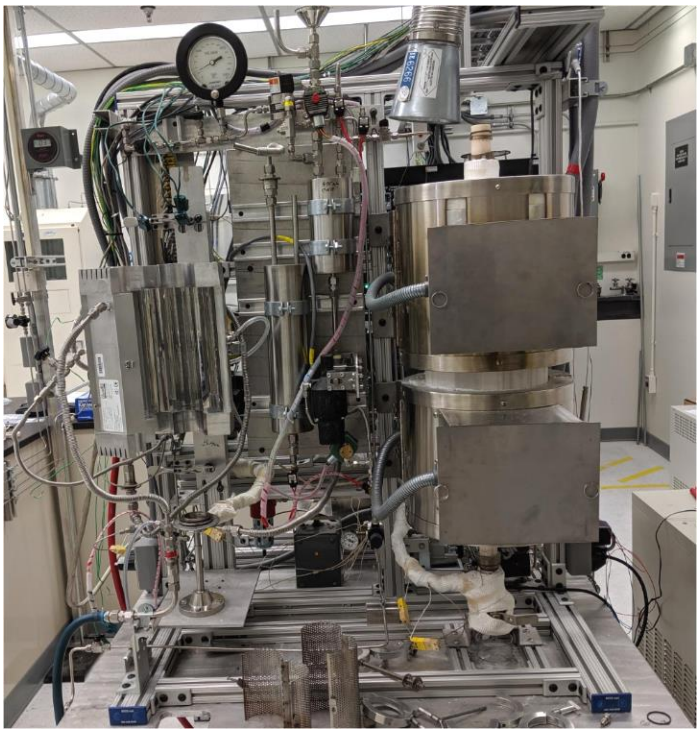

Figure 1. The Severe Accident Test Station (SATS) used to simulate design-basis loss of coolant accident (LOCA) conditions at ORNL.

Table 1. Composition of the nuclear-grade C26M FeCrAl cladding tubes used in this work.

Alloy	Fe	Cr	Al	Mo	Si	Y	Other
C26M	Bal.	11.9	6.2	1.98	0.2	0.03	<0.01 C<0.005 S

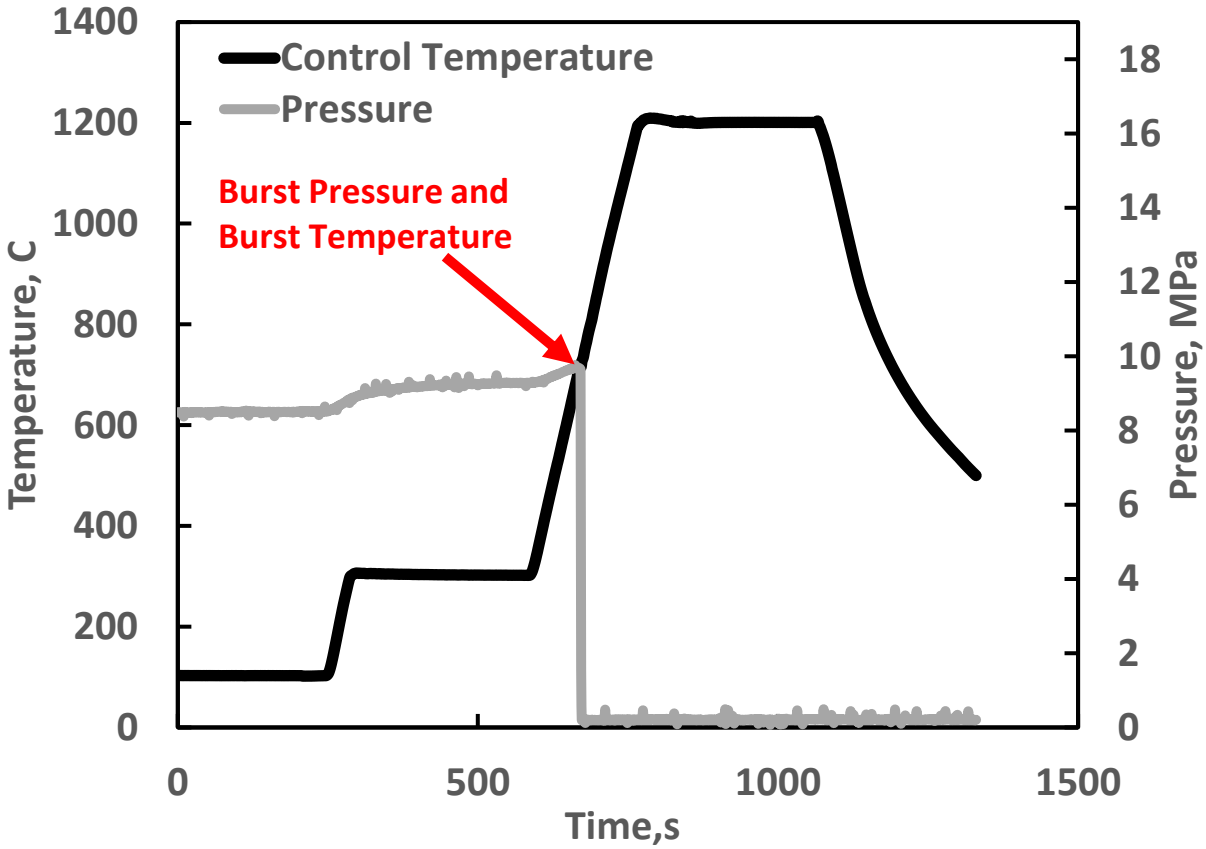

Figure 2. Typical temperature and pressure history of a design-basis LOCA event.

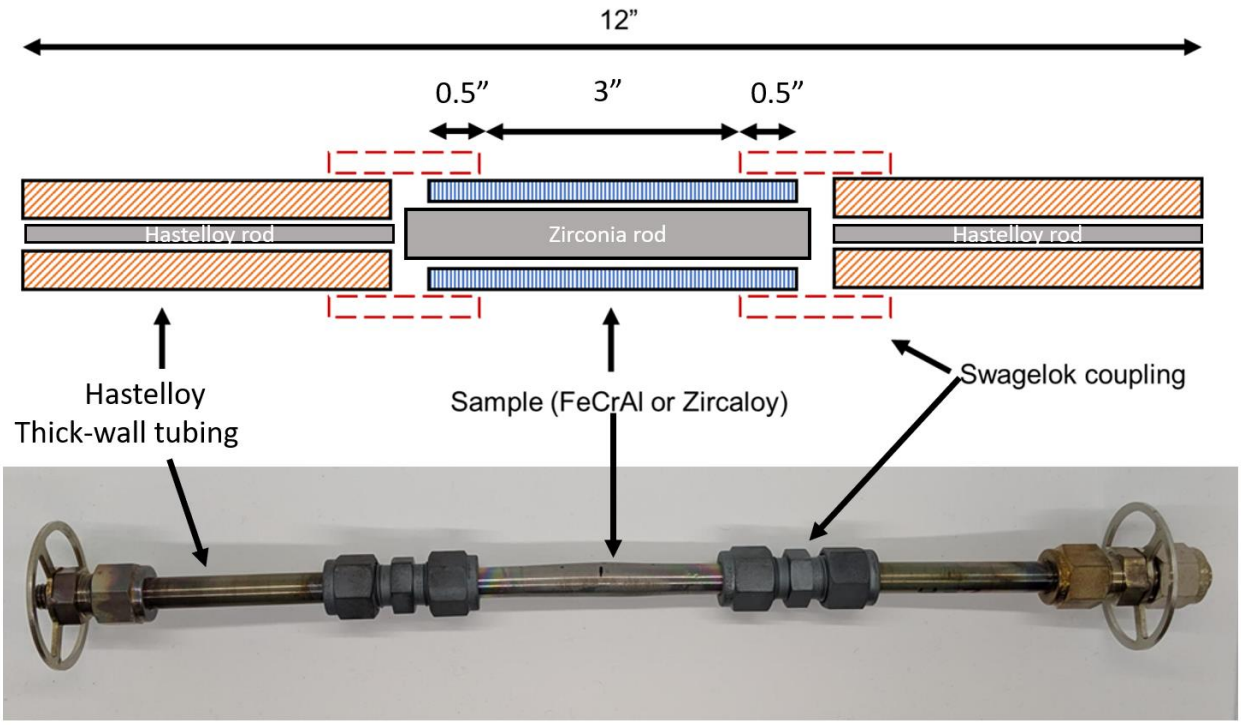

Figure 3. Setup for specimens shorter than the standard 12 inches.

2.2 SATS RESULTS WITH VARYING-LENGTH SPECIMENS

Tube specimens of lengths as short as 4 inches were tested at an initial pressure of 8.3 MPa (1,200 psi), and the results were compared to 12-inch data with the same material. The 4-inch specimens were sufficiently long to induce rupture, so more tests were performed at initial pressures of 3.8 and 5.9 MPa (550 and 850 psi respectively). Results of those tests are shown in Figure 4 below. Specimen lengths as short as 4 inches did not have a significant impact on burst location, pressure, temperature, or size, suggesting that it is an acceptable length for SATS specimens.

The specimen burst openings were measured after testing, and images were taken on the Keyence microscope. Burst measurement results are shown in Figure 5. The size of the burst opening was shown to be insensitive to specimen lengths as low as 4 inches. The burst width, burst height, and final tube OD at the burst were approximately constant at all specimen lengths. The burst length showed larger scatter, but it did not appear to correlate with specimen length. Previous burst measurements with the standard 12-inch LOCA specimen showed similar results, and their measurements were within the scatter of these shorter length specimen measurements [7].

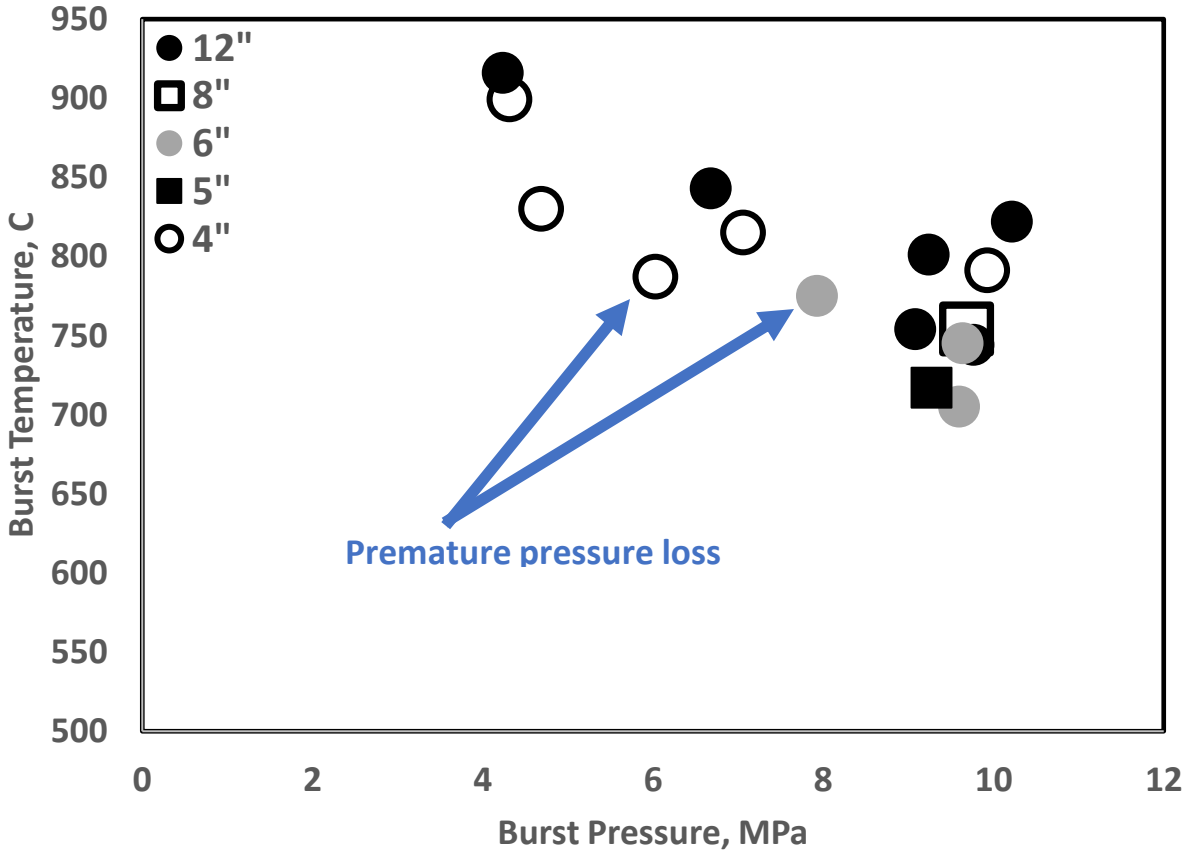

Figure 4. Burst temperature vs. burst pressure results of varying lengths of C26M2 FeCrAl SATS specimens (4-inch specimens appear to be within scatter and are still a valid specimen length).

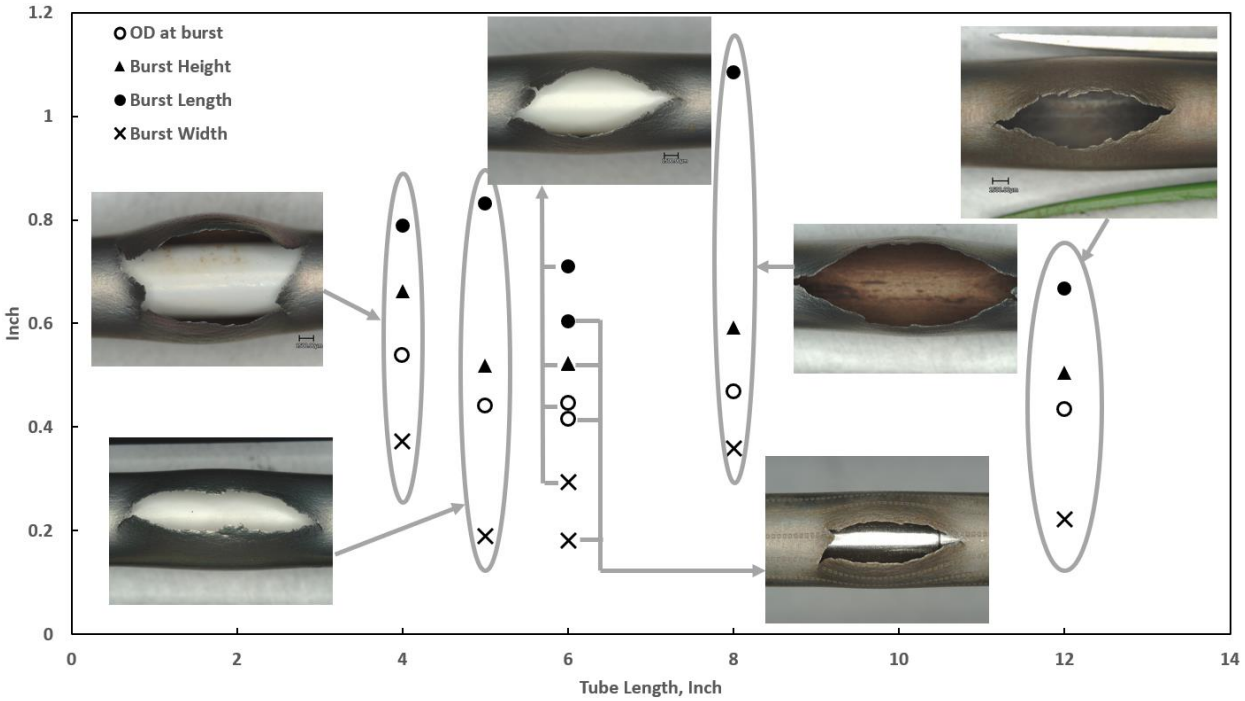

Figure 5. Images and measurements of the burst openings for varied-length specimens at an initial pressure of 8.3 MPa (1,200 psi). No correlation was shown between specimen length and burst measurements.

2.3 DIC TECHNIQUE WITH LASER-ENGRAVED SURFACES

A 6-inch FeCrAl tube specimen was engraved with 18 rows (20 degrees of rotation between each row) of a repeated square pattern in the axial direction. Each square was 400 × 400 µm, and the squares were spaced with 400 µm edge to edge. The row length was 60 mm. These squares were engraved with the laser at 20 kHz at 20 Watts. The engraving depth on this specimen post-SATS-test was measured to be less than 15 microns deep. An image of the engraved pattern on the tube's surface is shown in Figure 6a, and an image of the depth of the engraved square pattern is shown in Figure 6b.

a)

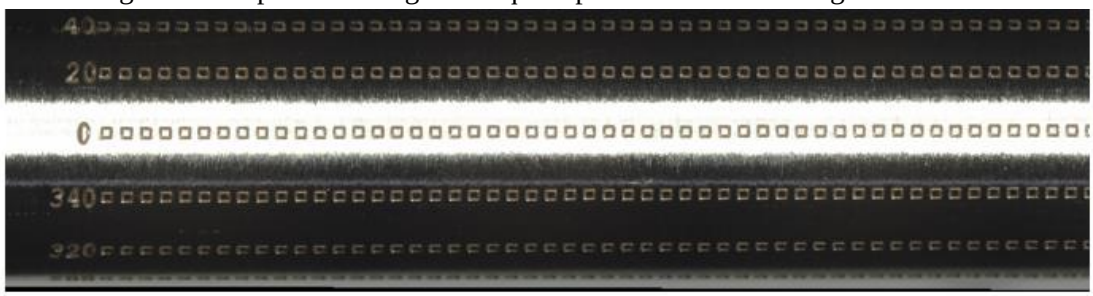

b)

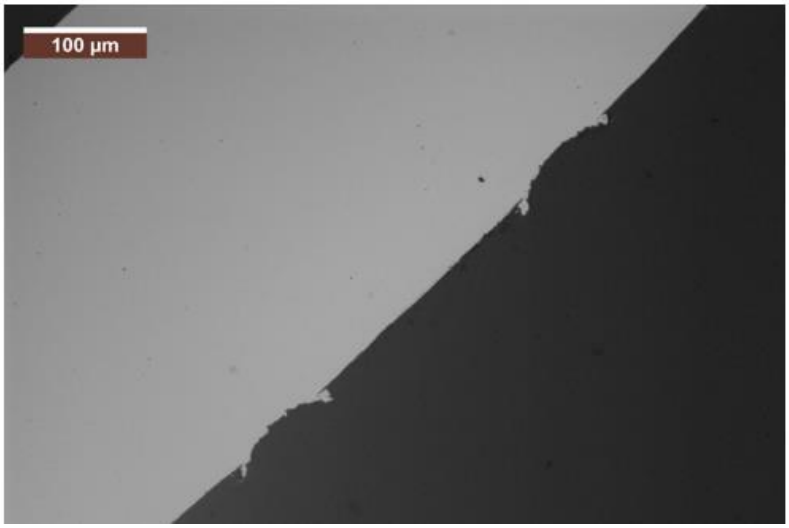

Figure 6. Image of the engraving pattern used for DIC strain calculations (a), and optical microscope image showing the depth of the square engraved pattern (b).

Three-dimensional microscope images were captured of the engravings at the burst location, at π/4 radians from the burst location in the circumferential direction and at π radians from the burst location in the circumferential direction before and after the LOCA test. Images of the burst location and results from DIC analysis at all three locations are shown in Figure 7. Axial strains at all orientations and hoop strains on the back of the specimen were calculated to be between 0 and 5%. As expected, hoop strain calculations increased near the location of the burst. Hoop strains pi/4 radians from the burst were calculated to be between 5 and 10%, and hoop strains at the burst location were calculated to be between 5 and 20%, with the maximum strain being closest to the burst's axial location. Due to the large rotation of the engraved square directly at the burst location, the DIC software could not analyze that specific axial location. DIC calculations were validated with direct measurements using the microscope's image analysis software taken on the engravings before and after the LOCA test. Those measurements were within the range of DIC calculated values. Furthermore, pre- and post-test measurements of the engravings nearest the burst location were averaged, and hoop strain was measured to be 77%. The technique proves to be effective at calculating specimen surface strains from a SATS LOCA burst.

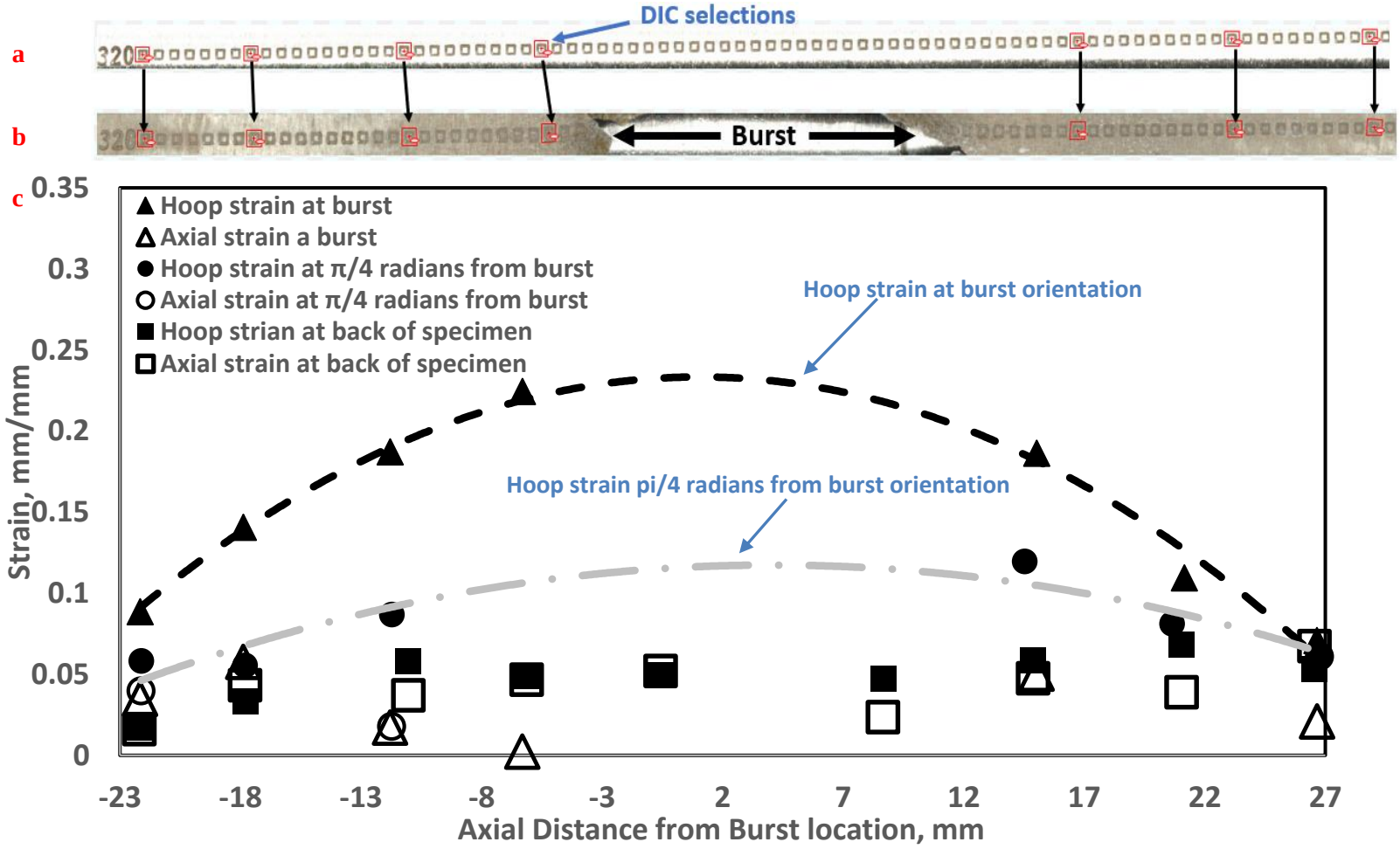

Figure 7. Image of engravings and DIC selection areas on FeCrAl tube surface before SATS test (a), where the DIC software traced the selected strain-measurement locations on the post-test image (b), and hoop strain results calculated from DIC software at different tube locations relative to burst location (c). A biaxial stress state was calculated on the opposite orientation of the burst with less biaxiality at the burst location

3. IRRADIATION TARGET DESIGN

3.1 DESIGN CONCEPT

Having shown 4-inch length cladding specimens to be viable for SATS LOCA experiments, efforts were initiated for the irradiation of such specimens in HFIR. The small "rabbit" capsules typically used for HFIR irradiations can only accommodate specimens up to around 2 inches long, so HFIR irradiations of 4-inch cladding specimens require a new full-length target design. A standard target is a sealed aluminum tube that is 23 inches long with a 0.53-inch inner diameter. In this experiment, the tube is loaded with four specimen assemblies 4 inches in length, as shown in Figure 8. Graphite spacers align the assemblies to be centered around the midplane of the reactor core, and a spring near the top accounts for axial expansion. Four specimen assemblies were chosen so that the dose variation in the center assemblies could be minimized without sacrificing the length of the specimens, the number of low dose variation samples, or the total amount of specimen material. Specifically, the center two specimens see a ~10% maximum variation in dose compared to a ~40% maximum variation for the outer two specimens. Note that these values are approximately halved if only including the center two inches of each specimen. This is important, as differential swelling is expected to lead to residual stresses in the irradiated material. Other assembly configurations have their own benefits but were found to be less attractive in general than the 4 × 4-inch case. For example, the 3 × 6-inch case has lower dose variation in the center specimen (5% vs. 10%) and a greater overall amount of specimen material (18-inches vs. 16-inches), but it only produces a single specimen with minimal dose variation per target as opposed to two specimens in the 4 × 4-inch case, and it also increases the dose variation in the top and bottom specimens (60% vs. 40%).

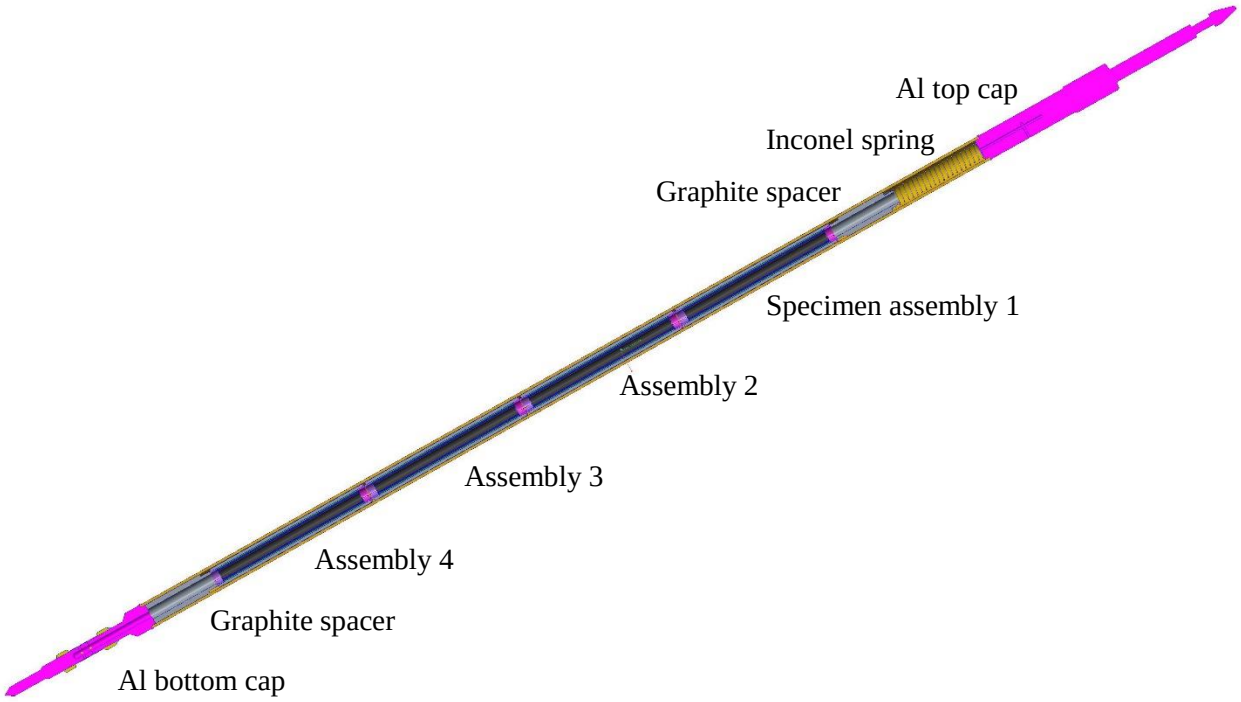

Figure 8. Design of the cladding irradiation experiment performed in HFIR at ORNL.

Moving radially from the outside in, a specimen assembly (shown in Figure 9) consists of a slightly tapered aluminum holder, a 4-inch length cladding specimen, and a graphite filler. The holder is tapered so the OD decreases at the axial ends of the holder to counteract the reduction in nuclear heating rates further away from the axial midplane of the reactor core. Reducing the holder diameter increases the gas gap between the holder and the target housing, which allows for a more uniform temperature throughout the length of the specimen. Figure 10 shows the axial variation in the holder diameter as well as the relative power factor, normalized so that the nuclear heating rate is equal to 1 at the axial midplane. The holders of the outer assemblies feature two tapers (i.e., the holder diameter follows one taper initially and then switches slopes approximately midway) instead of a single taper for the center positions. This is due to the power profile having a steeper slope in the end assemblies compared to the slope near the midplane. Within the graphite filler are four pieces of silicon carbide (SiC) passive thermometry which are held in place by curved SiC retainer springs. The thermometry can be evaluated using dilatometry post irradiation to estimate the temperature during operation [8]. On either end of each assembly, the internals are supported by molybdenum disks and titanium centering thimbles. The two outermost centering thimbles on each side of the assembly stack are flat on the top to rest on the graphite spacers, while the other thimbles feature tabs to minimize axial heat loss.

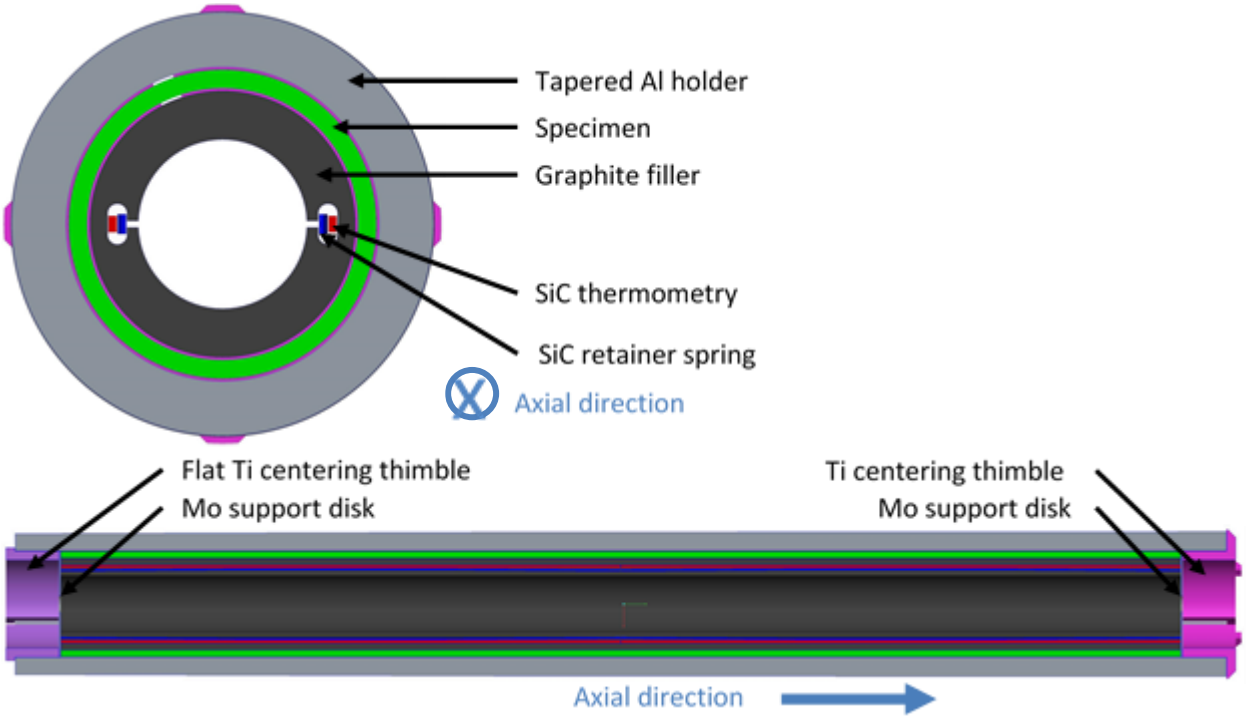

Figure 9. Cross sections of the new cladding specimen assembly design incorporated in the irradiation experiments shown in Figure 8. Note that the disks are hidden in the top-down section for clarity.

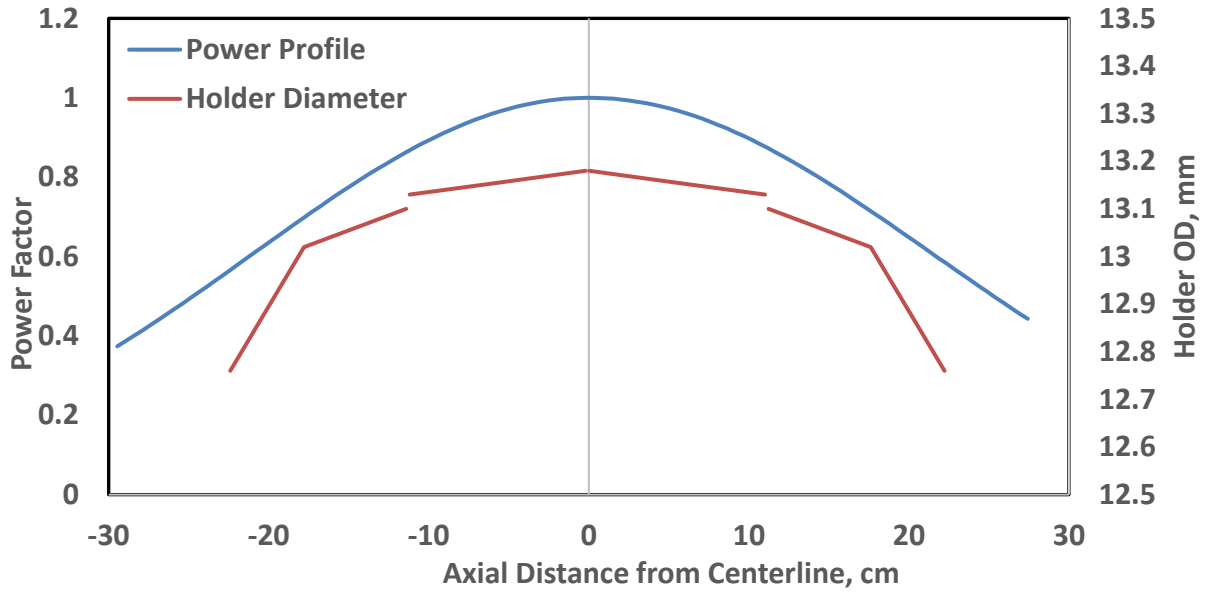

Figure 10. Tapered profile of the Al holder accounting for temperature changes from the power generation profile by decreasing the holder OD to improve thermal conductivity.

3.2 SETUP FOR THERMAL ANALYSIS OF IRRADIATION DESIGN

To determine the temperature distributions within the irradiation experiment, the ANSYS finite element software is used with custom, user-defined macros. Descriptions of these macros can be found in Design and Analysis Calculation (DAC) 11-13-ANSYS02, Rev. 6, which is available by request [9]. Likewise, temperature-dependent (and in the case of SiC, dose-dependent) material properties are calculated using a database of DACs maintained by the ORNL Nuclear Experiments and Irradiation Testing Group. These properties are obtained from CINDAS [10], MatWeb [11], and a variety of literature sources. Table 2 lists the previously approved DACs that were used in this calculation. Note that the modeled specimens can be FeCrAl, coated Zircaloy, SiC, or other materials of interest.

Heat generation rates (HGRs) and boundary conditions used in the design calculation can be found in Table 3. To optimize the holder diameters, the model is parameterized and used to construct a response surface with the ANSYS DesignXplorer software package. This is a fitted model of the response of the system to many inputs, and it allows for quick and accurate prediction of results. In the case of the cladding tube target irradiation, the holder diameters are the primary inputs, and the temperatures of the specimens are the outputs. By predicting these values, the temperature variation along the lengths of the specimens can be minimized while simultaneously achieving targeted average temperatures.

Table 2. Cladding tube irradiation materials and material property references

Part	Material	Reference DAC
Housing, holders	Aluminum	DAC-10-03-PROP_AL6061 [12]
Spacers, fillers	Graphite	DAC-10-15-PROP_POCO-GRAPHITE [13]
Specimen type 1	FeCrAl	DAC-16-02-PROP_FeCrAl [14]
Specimen type 2	Zircaloy	DAC-11-03-PROP_ZIRCALOY [15]
Specimen type 3, retainer springs, thermometry	Silicon carbide	DAC-10-06-PROP_SIC(IRR) [16]
Support disks	Molybdenum	DAC-10-11-PROP_MOLY [17]
Thimbles	Titanium	DAC-11-14-PROP_TI6AL4V [18]

3.3 RESULTS FROM THERMAL ANALYSIS

Temperature profiles for the specimens are presented in Figure 11 for the illustrative case of FeCrAl specimens with 17 × 17 array pressurized water reactor cladding geometry and a target temperature of 325°C. Note that results for SiC and coated Zircaloy specimens are not shown here for brevity. Table 4 shows the optimized holder ODs and specimen temperatures for each of the four assemblies. The holders are tapered between these diameters, so the edge holders have two slopes, while the center holders have only one. Furthermore, the holders were constrained to be symmetric about the midplane. Both decisions were made to improve the ease of manufacturing, although results could be further enhanced by increasing the degrees of freedom. However, even with these constraints, the average temperatures in the specimens are all within 3°C of the target temperature, and there is a ≤ 2% difference between any of the extreme values and the target. Additionally, preliminary safety calculations show a sufficient margin to melt in all components. This suggests that full-length targets should be a viable path for irradiating a variety of cladding tube specimens in HFIR.

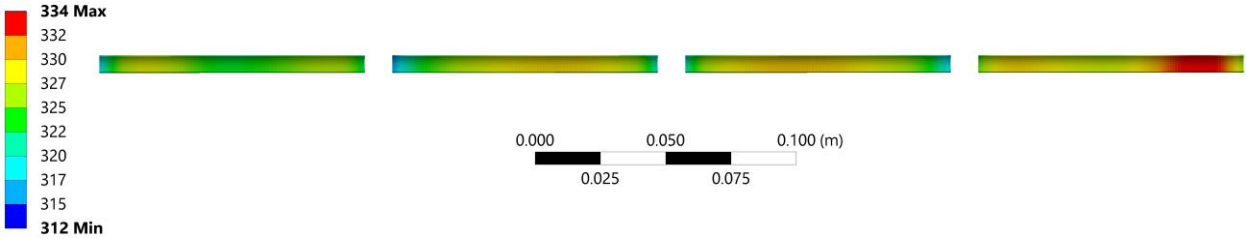

Figure 11. Temperatures (in °C) of the FeCrAl cladding tube specimens during HFIR irradiation using the new target design (results obtained from ANSYS simulations).

Table 3. Optimized holder diameters (inputs) and FeCrAl specimen temperatures (outputs) for ANSYS simulations

Spec.	Top OD (mm)	Mid. OD (mm)	Bot. OD (mm)	Tavg (°C)	Tmin (°C)	Tmax (°C)	Tmax-Tmin (°C)
1	12.76	13.02	13.10	328	321	334	13
2	13.13	---	13.18	325	314	330	16
3	13.18	---	13.13	324	312	330	18
4	13.10	13.02	12.76	323	316	328	12

Table 4. Cladding tube irradiation thermal boundary conditions

Parameter	Value	Reference
Convective heat transfer coefficient	48.8 kW/m^2·K	Average of values [19–21]
Bulk coolant temperature	64.3°C	Average of values [19-21]
Power profile correlating parameter	30.07 cm	C-HFIR-2012-035 Rev. 0 [22]
Peak HGR for aluminum	31.3 W/g	C-HFIR-2012-035 Rev. 0 [22]
Peak HGR for FeCrAl	33.5 W/g	C-HFIR-2017-011 Rev. 0 [23]
Peak HGR for graphite	32.5 W/g	C-HFIR-2012-035 Rev. 0 [24]
Peak HGR for molybdenum	46.1 W/g	C-HFIR-2013-003 Rev. 0[25]
Peak HGR for silicon carbide	29.2 W/g	C-HFIR-2017-011 Rev. 0 [26]
Peak HGR for titanium	35.2 W/g	C-HFIR-2013-003 Rev. 0 [27]
Peak HGR for Zircaloy	52.3 W/g	C-HFIR-2017-011 Rev. 0 [28]

4. CONCLUSIONS

This research was performed to study the length dependence of nuclear-grade FeCrAl cladding required to run a LOCA relevant experiment in the Severe Accident Test Station (SATS). To accomplish this, experiments with varied lengths and pressures were performed using unirradiated FeCrAl thin-walled tube specimens. The SATS simulates a LOCA by increasing the temperature of an internally pressurized tube in a steam environment in a postulated design basis accident. This increasing temperature consequently increases the internal pressure and hoop stress on the tube specimen until it bursts. Tube performance was quantified by the burst temperature, burst pressure, hoop stresses, and burst characteristics of the tube specimen. Burst measurements were obtained with a micrometer, and images were obtained with a Keyence microscope. Burst results from the various lengths of tube specimens were compared, and it was demonstrated that specimens as short as 4 inches in length were within the scatter of results obtained using the standard 12-inch specimens for C26M FeCrAl material.

DIC analysis was performed with a laser-engraved 6-inch specimen. Analysis showed the technique to be effective at calculating strains on the LOCA burst specimens with FeCrAl cladding material. Further research is recommended to improve the overall output of the technique. Specifically, developing an engraving pattern that can calculate strains continuously across the axial length of the tube without negatively affecting mechanical performance would significantly improve the technique's output. Furthermore, more testing and material analyses are recommended. Tube cross-sections may be prepared and analyzed with EBSD scanning to investigate the microstructure and grain morphology evolution from laser engraving as well as during high-temperature deformation and burst.

From the conclusions of the length-dependence studies, a new cladding tube irradiation target was designed to accommodate 4-inch long specimens. A single HFIR target with four 4-inch specimens will produce two dose conditions: one for the two specimens in the centerline region with minimal dose variation across the specimens, and one for the specimens loaded in the outermost target positions with larger dose variations. ANSYS modeling software was used to determine the appropriate tapered outside diameter of the Al holder to optimize the irradiation target's thermal performance during HFIR irradiations based on the reactor's known power profile. Simulation results with the same FeCrAl material from LOCA burst tests determined that all 4-inch specimen assemblies would experience excellent temperature uniformity and accuracy during the HFIR irradiation run. These results indicate the full-length HFIR target accommodating 4-inch long cladding specimens is a viable design for accelerated irradiation testing of thin-walled cladding tube segments.

5. REFERENCES

[1] S. J. Zinkle, K. A. Terrani, J. C. Gehin, L. J. Ott, and L. L. Snead, 2014. Accident Tolerant Fuels for LWRs: A Perspective, J. Nucl. Mater. 448, 374–379.

[2] K. A. Terrani, 2018. Accident Tolerant Fuel Cladding Development: Promise, Status, and Challenges, J. Nucl. Mater. 501, 13–30.

[3] K. G. Field, M. A. Snead, Y. Yamamoto, and K. A. Terrani, 2018. Handbook on the Material Properties of FeCrAl Alloys for Nuclear Power Production Applications, ORNL/SPR-2018/905.

[4] B. A. Pint, 2018. Steam Oxidation, Burst and Critical Heat Flux Testing of FeCrAl Cladding in the SATS, ORNL/LTR-2018/530.

[5] Y. Yan, T. A. Burtseva, and M. C. Billone, 2004. LOCA Integral Test Results for High-Burnup BWR Fuel, NUREG/CP-0192, 111–158.

[6] D. A. Powers and R. O. Meyer, 1980. Cladding Swelling and Rupture Models for LOCA Analysis, NUREG-0630.

[7] C. P. Massey, K. A. Terrani, S. N. Dryepondt, B. A. Pint, 2016. Cladding Burst Behavior of Fe-based Alloys Under LOCA, J. Nucl. Mater. 470, 128-138.

[8] K. G. Field et al., 2019. "Evaluation of the continuous dilatometer method of silicon carbide thermometry for passive irradiation temperature determination," *Nuclear Instruments and Methods in Physics Research B*, **445**, pp. 46–56.

[9] J. L. McDuffee, 2016. "Solve Macros for ANSYS Finite Element Models With Contact Elements," DAC-11-13-ANSYS02, Rev. 6, Oak Ridge National Laboratory, Oak Ridge, TN.

[10] *CINDAS, LLC: Global Benchmark for Critically Evaluated Materials Properties Data*, Available from: http://cindasdata.com.

[11] *MatWeb: Material Property Data*, Available from: http://matweb.com/.

[12] J. L. McDuffee, 2013. "Thermophysical Properties for AL6061," DAC-10-03-PROP_AL6061, Rev. 2, Oak Ridge National Laboratory, Oak Ridge, TN.

[13] J. L. McDuffee, 2013. "Thermophysical Properties for POCO Graphite," DAC-10-15-PROP_POCO-GRAPHITE, Rev. 1, Oak Ridge National Laboratory, Oak Ridge, TN.

[14] C. M. Petrie, 2016. "Thermophysical Properties for FeCrAl," DAC-16-02-PROP_FeCrAl, Rev. 0, Oak Ridge National Laboratory, Oak Ridge, TN.

[15] J. L. McDuffee, 2016. "Thermophysical Properties for Zircaloy," DAC-11-03-PROP_ZIRCALOY, Rev. 2, Oak Ridge National Laboratory, Oak Ridge, TN.

[16] J. L. McDuffee, 2013. "Thermophysical Properties for Irradiated SiC," DAC-10-06-PROP_SIC(IRR), Rev. 3, Oak Ridge National Laboratory, Oak Ridge, TN.

[17] J. L. McDuffee, 2013. "Thermophysical Properties for Molybdenum," DAC-10-11-PROP_MOLY, Rev. 1, Oak Ridge National Laboratory, Oak Ridge, TN.

[18] J. L. McDuffee, 2013. "Thermophysical Properties for Titanium Alloy Ti-6Al4V," DAC-11-14-PROP_TI6AL4V, Rev. 1, Oak Ridge National Laboratory, Oak Ridge, TN.

[19] S. H. Kim, 2004. "Safety Calculations for JP-27 Experiment," C-HFIR-2004-006, Rev. 0, Oak Ridge National Laboratory, Oak Ridge, TN.

[20] S. H. Kim, 2004. "Safety Calculations for JP-28 Experiment," C-HFIR-2004-024, Rev. 0, Oak Ridge National Laboratory, Oak Ridge, TN.

[21] S. H. Kim, 2004. "Safety Calculations for JP-29 Experiment," C-HFIR-2004-025, Rev. 0, Oak Ridge National Laboratory, Oak Ridge, TN.

[22] J. L. McDuffee, 2012. "Heat Generation Rates for Various Rabbit Materials in the Flux Trap of HFIR," C-HFIR-2012-035, Rev. 0, Oak Ridge National Laboratory, Oak Ridge, TN.

[23] C. R. Daily, 2018. "Heat Generation Rates for Various Fe-Cr-Al, Inconel, and Zircaloy Samples to be Irradiated in the HFIR Flux Trap," C-HFIR-2017-011, Rev. 0, Oak Ridge National Laboratory, Oak Ridge, TN.

[24] C. R. Daily, 2013. "Heat Generation Rates for Various Titanium and Silicon Compounds in the Flux Trap of HFIR," C-HFIR-2013-003, Rev. 0, Oak Ridge National Laboratory, Oak Ridge, TN.